Journal of Naval Architecture and Marine Engineering
December, 2021
http://dx.doi.org/10.3329/jname.v18i2.55253 *http://www.banglajol.info*

EFFECT OF JOULE HEATING ON STEADY MHD CONVECTIVE MICROPOLAR FLUID FLOW OVER A STRETCHING/SHRINKING SHEET WITH SLIP

A. P. Baitharu[1], S. N. Sahoo[2], G. C. Dash[3]

[1]Department of Mathematics, College of Engineering and Technology, Bhubaneswar-751029, Odisha, India, Email: abaitharu2@gmail.com

[2]Department of Mathematics, ITER, Siksha 'O' Anusandhan (Deemed to be University), Bhubaneswar-751030, Odisha, India, Email: sachimath1975@gmail.com

[3]Department of Mathematics, ITER, Siksha 'O' Anusandhan (Deemed to be University), Bhubaneswar-751030, Odisha, India, Email: gcdash45@gmail.com

Abstract:

The effect of Joule heating on the steady two-dimensional flow of an incompressible micropolar fluid over a flat deformable sheet is analyzed when the sheet is stretched with a slip in its own plane. The effects of first and second-order slips with dissipative heat energy are considered in the present study. The numerical solution to coupled non-linear differential equations is obtained using the Runge-Kutta method of fourth-order with shooting technique. The important findings of the present study are due to the shrinking effect, temperature increases more than that of stretching which is analogous to contraction and expansion forming the basis of a heat engine (transporting thermal energy to mechanical energy); the thermal buoyancy overpowers the inertia force; the second-order slip is favorable for flow stability in both stretching and shrinking of the deformable surface.

Keywords: MHD flow, micropolar fluid, Joule heating, Newtonian heating, slip flow

NOMENCLATURE

x, y	horizontal and transverse directions respectively (m)	M	dimensionless magnetic parameter
u, v	horizontal and vertical velocity components respectively(ms^{-1})	Pr	Prandtl number
u_w	velocity of the sheet(ms^{-1})	Gr_x	local Grashof number
n	strength of concentration of microelements	Re_x	local Reynolds number
g	gravitational acceleration(ms^{-2})	C_{fx}	local skin friction coefficient
T	temperature of the fluid(K)	M_x	local wall couple stress
T_∞	free stream temperature(K)	m_w	wall couple stress (Nm^{-2})
B_0	magnetic field strength($kgA^{-1}s^{-2}$)	Nu_x	local Nusselt number
a	stretching rate(s^{-1})	q_w	wall heat flux (kgs^{-3})
k	thermal conductivity($Js^{-1}m^{-1}K^{-1}$)	Bi	Biot number
j	microinertia per unit mass(m^2)	***Greek symbols***	
f_w	dimensionless suction or injection parameter	μ	dynamic viscosity ($kgm^{-1}s^{-1}$)
Q_0	volumetric rate of heat generation ($JK^{-1}m^{-3}$)	ν	kinematic viscosity of the fluid(m^2s^{-1})
s	stretching/shrinking constant	σ	electrical conductivity($s^3A^2kg^{-1}m^{-3}$)
v_0	suction/injection velocity (ms^{-1})	ρ	density of the fluid(kgm^{-3})
h_s	surface heat transfer coefficient ($Jm^{-2}s^{-1}K^{-1}$)	χ	microrotation viscosity($kgm^{-1}s^{-1}$)
K	dimensionless material parameter	β_T	coefficient of thermal expansion(K^{-1})
l	constant	ω	micro-rotational velocity(ms^{-1})
Ec	Eckert number	γ	spin gradient viscosity coefficient($kgms^{-1}$)
k_n	Knudsen number	ψ	stream function(m^2s^{-1})

1813-8535 (Print), 2070-8998 (Online) Received on: August 2021

d	molecular mean free path(m)	ε	momentum accommodation coefficient
A	constant coefficient for mean free path(m)	θ	dimensionless temperature
B	square of constant coefficient for mean free path(m^2)	λ	buoyancy parameter(N)
C_p	specific heat at constant pressure($Jkg^{-1}K^{-1}$)	η	dimensionless variable
f	dimensionless velocity	α	dimensionless first order slip flow parameter
h	dimensionless micro-rotational velocity	δ	dimensionless Newtonian heating parameter
Q	heat generation (>0) or the heat absorption (<0) parameter	β	dimensionless second order slip flow parameter

1. Introduction

Theoretical research conducted on micropolar fluids receives considerable attention since last few years as the Newtonian fluid is not capable to describe the fluid flows with suspended particles. The micropolar fluids are defined as fluids with microstructure that belong to a single class of stress tensor (non-symmetrical fluids). In physical terms, it is called the fluids that are comprised of suspended particles oriented randomly in a viscous medium. The micropolar fluids are the non-Newtonian fluids with short-rigid elements of cylindrical shape or dumb-bell molecules, fluid suspensions, polymer fluids, and animal blood. Some particular smoke or dust particles present in the gas might also be modeled as per the dynamics of the micropolar fluid. Some interesting applications of the present study are: thinning of the velocity boundary layer which is useful in maintaining laminarity (avoiding turbulence), thickening of the thermal boundary layer which quickens the process of thermal diffusion, cooling of deformable surface required for the design of heat exchanger. Bakar (2011) has studied the unsteady MHD flow of a micropolar fluid as well as mass transfer with a constant source of heat in a rotating frame of reference considering first-order chemical reaction in the presence of constant suction and an oscillatory-plate velocity. Mohamed (2013) analyzed the convective micropolar fluid flow over a time-dependent stretching plate with viscous dissipation and observed that the micropolar parameter enhances the rate of heat transfer opposing the flow in both forced and mixed convection regimes and reducing the flow in free convection regime. Sheri and Shamshuddin (2015) have also studied heat and mass transfer for the MHD flow of micropolar fluid with chemical reactions and viscous dissipation. Rout et al. (2016) have studied the effect of chemical reaction on the boundary layer flow of an electrically conducting micropolar fluid past a vertical plate subject to a transverse magnetic field with variable wall concentration and temperature. Animasaun (2017) has analyzed the heat and mass transfer in a micropolar fluid flow towards a stagnation point considering temperature-dependent fluid viscosity and a constant vortex viscosity.

In the past few decades, the micropolar fluid flow past a stretching sheet is a subject of prime investigation due to various applications in the industrial fields like metal tinning and annealing, crystal growing, paper production etc. Pal and Mondal (2010) have investigated the impact of viscosity on the non-Darcy magnetohydrodynamics mixed convective heat transfer on a porous medium, considering the non-uniform heat sink or source and the Ohmic dissipation. Ahmad et al. (2013) have studied numerically the micropolar fluid flow and heat transfer past a non-linearly stretching surface, taking into account the effect of viscous dissipation. Their study reveals that the increase in non-linear stretching parameter decreases the magnitude of Nusselt number and coefficient of skin friction, but the reverse effect is observed with an increase in the material parameter, keeping the stretching parameter fixed. Further Turkyilmazoglu (2014) studied the flow of micropolar fluids as well as heat transfer over the permeable shrinking sheet. The significance of heat transfer and boundary layer flow of micropolar fluid on a permeable sheet shrinking exponentially was analyzed by Aurangzaib et al. (2016). Pal and Mandal (2017) studied the MHD micropolar nanofluid flow over a stretching sheet with thermal radiation and a non-uniform heat sink or source. The Runge-Kutta-Fehlberg method with shooting technique was used to obtain the numerical solution. Pothanna et al. (2016), (2017, and (2019) have investigated the steady/unsteady flow of thermo-viscous incompressible fluid flow in different geometries. In some of the study, they have solved the boundary value problems using both analytical and numerical methods and found excellent agreement. They observed that the velocity profiles are shifted at a faster rate due to the increase in Darcy friction offered by the medium to the flow. They mentioned that the external forces generated are perpendicular to the flow direction and this is the special feature of the thermo-viscous fluid. Mebarek-Oudina et al. (2020) have analyzed the MHD natural convection in an upright porous cylindrical annulus filled with magnetized nanomaterial is made by using the specificity of nanoliquids to improve the phenomenon of

heat transport. They observed that the transferred thermal flux, in laminar natural convection, increases with the growth of the nanoparticle concentration, the Darcy number, the porosity, the Rayleigh number, and the length of the source. In a number of engineering usages, it was noticed that the particles in the fluid closer to a solid surface, slip along the surface because of its finite tangential velocity. This usually happens in the case of thin liquid and gas. Such a domain of flow is known as the slip-flow regime with shear stress varies with slip velocity. Such effects can never be ignored. The studies of slip-flows have various applications in engineering and technology like polishing the artificial heart valves and internal cavities, refrigerating the coils, transmission lines, etc. Mostafa et al. (2012) have studied heat transfer on MHD micropolar fluid flow over a stretching surface with slip velocity and heat absorption or generation. A time-independent mixed convective stagnation-point flow with second order slip past a vertical flat surface was analyzed by Rosca and Pop (2013). Sahoo and Dash (2012) have analyzed the influence of heat and mass transfer on magnetohydrodynamics convective boundary layer flow past a stretching wall embedded in a porous medium in the presence of the magnetic field of uniform strength and heat source. Sharma et al. (2016) studied the time-independent micropolar fluid flow past a shrinking or a stretching sheet with stagnation point considering the second-order slip velocity. Ibrahim (2017) has examined the effect of magnetic field and second-order slip on the boundary layer flow of micropolar fluid on a stretching surface. Kamran and Wiwatanapataphee (2018) and Kamran (2018) have analyzed the effects of Newtonian heating and chemical reaction on a steady convective micropolar fluid flow taking into account the second-order slip at the bounding surface. Khan et al. (2020) analyzed the heat and mass transfer effect in a doubly stratified medium of mixed convective flow with viscous dissipation. They have considered hyperbolic tangent fluid with chemical reaction and thermal radiation and observed that the skin friction coefficient decreases with the increase in power-law index. Again, Khan et al. (2021) have considered chemically reactive MHD Jeffery fluid flows with solar radiation over a non-uniform stretching sheet of variable thickness. Their study reveals a bi-folded behavior of velocity field due to the variable thickness of the sheet. It is also noticed that with the increase of Deborah's number the transverse and axial velocities are increasing but the reverse effect has been marked on the temperature and concentration distribution.

Many authors have neglected dissipations of thermal energy such as viscous and Joulean dissipations. Kamran (2018) also neglected viscous dissipation in his study. It is important to note that, even if there is no heat transfer to a body in a flow, a thermal boundary layer is formed at the boundary surface (Schlichting and Gersten (1999)). Therefore, in the present analysis, we have studied a conducting fluid flow under the influence of the external magnetic field generating a resistive electromagnetic force in the momentum transport equation. We have also considered both viscous and Joulean dissipations which contribute substantially to the velocity and thermal boundary layer structure. One vital aspect of the present study is to account for the slips at the boundary. Usually, a viscous fluid sticks to the boundary, i.e. there is no slip of the fluid at the boundary. In this context Beavers and Joseph (1967) pointed out that there may be a partial slip between fluid at the boundary. Another aspect of the present study is that it takes care of both stretching and shrinking whereas other studies such as Mohapatra and Gupta (2002), Mohapatra et al. (2007), Mishra and Sinha (2013), Baitharu et al. (2020), Swain et al. (2021) and many others have studied only stretching of the surface due to a mathematical impasse in defining similarity variables while pursuing similarity solution, but in the present study, both stretching/shrinking cases have been considered. The expansion and contraction serve as fundamental bases in the design of heat engines transferring thermal energy to mechanical energy. In view of the above discussion, we have been motivated to consider the following aspects in our present study:

(i) the dissipation of heat energy due to resistance offered by viscosity in momentum transport processes in the magnetohydrodynamics flow domain as well as by permeating flow of current in the conductor.

(ii) an additional body force (Lorentz force) due to the applied transverse magnetic field.

These aspects were not attended to while studying velocity and thermal slips in a micropolar fluid flow. Further, the study takes care of cross-flow (suction/injection), a preventive measure to the growth of the boundary layer.

2. Formulation of the Problem

Let us consider a two-dimensional, time-independent (steady), incompressible, electrically conducting, convective, and dissipative micropolar fluid flow with slip over a permeable stretching or shrinking sheet. The *x*-axis is taken along the stretching sheet and the *y*-axis is normal to it. The velocity of the sheet along the x-axis is $u = u_w(x) = ax$, where a is the stretching rate constant, a real number. The acceleration due to gravity g, is acting downward. Newtonian heating has been introduced in the thermal boundary condition.

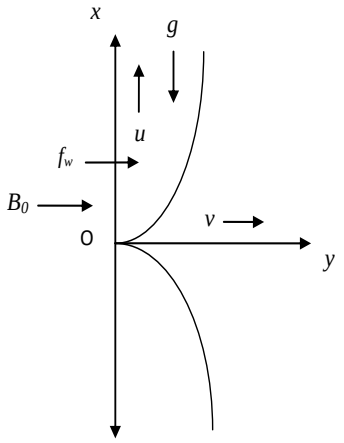

Fig. 1: Flow geometry

Under the usual Boussinesq and thermal boundary layer approximations, two-dimensional boundary layer equations for the electrically conducting micropolar fluid flow with boundary conditions following Kamran (2018) are given by

$$\frac{\partial u}{\partial x}+\frac{\partial v}{\partial y}=0, \tag{1}$$

$$u\frac{\partial u}{\partial x}+v\frac{\partial u}{\partial y}=\frac{\mu+\chi}{\rho}\left(\frac{\partial^2 u}{\partial y^2}\right)+g\beta_T(T-T_\infty)+\frac{\chi}{\rho}\left(\frac{\partial \omega}{\partial y}\right)-\frac{\sigma B_0^2 u}{\rho} \tag{2}$$

$$u\frac{\partial \omega}{\partial x}+v\frac{\partial \omega}{\partial y}=\frac{\gamma}{\rho j}\left(\frac{\partial^2 \omega}{\partial y^2}\right)-\frac{\chi}{\rho j}\left(2\omega+\frac{\partial u}{\partial y}\right) \tag{3}$$

$$u\frac{\partial T}{\partial x}+v\frac{\partial T}{\partial y}=\frac{k}{\rho C_p}\left(\frac{\partial^2 T}{\partial y^2}\right)+\frac{Q_0}{\rho C_p}(T-T_\infty)+\frac{\sigma B_0^2}{\rho C_p}u^2+\frac{(\mu+\chi)}{\rho C_p}\left(\frac{\partial u}{\partial y}\right)^2 \tag{4}$$

$$\left.\begin{array}{l} y=0 \;\; : u=su_w(x)+u_{\text{slip}},\; v=v_0,\; \omega=-n\dfrac{\partial u}{\partial y}, k\dfrac{\partial T}{\partial y}=-h_s T \\ y\to\infty: u\to 0, \omega\to 0,\; T\to T_\infty \end{array}\right\}, \tag{5}$$

where $\gamma=(\mu+\chi/2)j=\mu(1+K/2)j$, $K=\chi/\mu$ and $j=\nu/a$.

Here $v_0>0$ and $v_0<0$ represent the suction and injection velocity respectively. The microrotation parameter n lies between 0 and 1 i.e. $0\le n\le 1$. When n = 0, the microelements are unable to rotate and imposes strong concentrations at the stretching sheet. For n = 1/2, the skew-symmetric part of the stress tensor disappears and it indicates the fragile concentration of microelements. For n = 1, the flow is turbulent. The slip velocity of the shrinking $(s<0)$ or stretching $(s>0)$ sheet is given by

$$u_{slip}=\frac{2}{3}\left(\frac{3-\varepsilon l^3}{\varepsilon}-\frac{3}{2}\left(\frac{1-l^2}{k_n}\right)\right)d\frac{\partial u}{\partial y}-\frac{1}{4}\left(l^4+\frac{2}{k_n^2}\left(1-l^2\right)\right)d^2\frac{\partial^2 u}{\partial y^2}=A\frac{\partial u}{\partial y}+B\frac{\partial^2 u}{\partial y^2},$$

where $l\in\{\min(1/k_n,1)\}$ which implies $0<l\le 1$ for all k_n (Knudsen number). The momentum accommodation coefficient ε lies between 0 and 1 i.e. $0\le\varepsilon\le 1$ and d is the molecular mean free path which is always positive.

3. Solution of the Problem

Introducing the stream function $\psi(x,y)$ such that $u=\frac{\partial\psi}{\partial y}$ and $v=-\frac{\partial\psi}{\partial x}$ and the similarity variables such as $\eta=\sqrt{a/\nu}\,y, \psi=\sqrt{a\nu}\,xf(\eta),\ \omega=\sqrt{a/\nu}\,axh(\eta), \theta(\eta)=\frac{T-T_\infty}{T_\infty}$, the governing equations (2), (3) and (4) reduce to

$$(1+K)f'''-(f')^2+ff''-Mf'+\lambda\theta+Kh'=0, \tag{6}$$

$$(1+K/2)h''-hf'+h'f-K(2h+f'')=0, \tag{7}$$

$$\theta''+Pr\,f\theta'+Q\,Pr\,\theta=-PrEc[(1+K)(f'')^2+M(f')^2]. \tag{8}$$

The corresponding boundary conditions are

$$\left.\begin{array}{l}\eta=0\ : f=f_w,\ f'=s+\alpha f''+\beta f''', h=-n f'', \theta'=-\delta(1+\theta)\\ \eta\to\infty: f'\to 0,\ h\to 0, \theta\to 0\end{array}\right\} \tag{9}$$

The dimensionless parameters are $\lambda=Gr_x/Re_x$, $Gr_x=g\beta_T T_\infty x/a\nu$, $Re_x=ax^2/\nu$, $Q=Q_0/a\rho C_p$, $Pr=\mu C_p/k$, $f_w=-(a\nu)^{-1/2}v_0$, $M=\sigma B_0{}^2/\rho a$, $Ec=a^2x^2/C_pT_\infty$, $\alpha=A\sqrt{a/\nu}>0$, $\beta=Bi/\nu<0$ and $\delta=\sqrt{\nu/a}\,h_s/k$.

The local skin friction coefficient (C_{f_x}), wall couple stress (M_x) and Nusselt number (Nu_x) are given by

$$C_{f_x}=\frac{\tau_{wx}}{\rho(u_w(x))^2}\ \text{, where}\ \tau_{wx}=(\mu+\chi)\frac{\partial u}{\partial y}+\chi\omega\Big]_{y=0}=(1+K-nK)f''(0)/Re_x^{1/2} \tag{10}$$

$$\Rightarrow C_{f_x}Re_x^{1/2}=(1+K-nK)f''(0) \tag{11}$$

$$M_x=\frac{-m_w}{\rho x(u_w(x))^2}\ \text{, where}\ m_w=(\mu+\chi/2)j\frac{\partial\omega}{\partial y}\Big]_{y=0}, \tag{12}$$

$$\Rightarrow M_xRe_x=-(1+K/2)h'(0). \tag{13}$$

$$Nu_x=\frac{-xq_w}{k_f(T-T_\infty)}\ \text{, where}\ q_w=k_f\frac{\partial T}{\partial y}\Big]_{y=0}, \tag{14}$$

$$\Rightarrow Nu_xRe_x^{-1/2}=\delta\left(1+1/\theta(0)\right). \tag{15}$$

4. Methodology

The set of nonlinear coupled ordinary differential equations (6)-(8) with boundary condition (9) are solved by fourth order Runge-Kutta method with shooting technique using MATLAB's built-in solver bvp4c. For the present computation, we choose the step size $\Delta\eta=0.01$ and the rate of convergence criteria 10^{-6}. The transformed system of 1st order equations are

$$f=y_1, f'=y_1'=y_2, f''=y_2'=y_3, h=y_4, h'=y_4'=y_5, \theta=y_6, \theta'=y_6'=y_7,$$

$$f'''=y_3'=\{1/(1+K)\}\left(y_2{}^2-y_1y_3+My_2-\lambda y_6-Ky_5\right),$$

$$h''=y_5'=\{2/(2+K)\}\left(y_4y_2-y_5y_1+K(2y_4+y_4)\right),$$

$$\theta''=y_7'=-Pry_1y_7-QPry_6-PrEc\left\{(1+K)y_3{}^2+My_2{}^2\right\}.$$

subject to the subsequent conditions,

$$y_1(0)=f_w, y_2(0)=s+\alpha y_3(0)+\beta\{1/(1+K)\}\left(y_2{}^2-y_1y_3+My_2-\lambda y_7-Ky_6\right),$$

$$y_4(0)=-ny_3(0), y_7(0)=-\delta(1+y_6(0)),$$

$y_2(\eta) \to 0, y_4(\eta) \to 0, y_6(\eta) \to 0$ as $\eta \to \infty$

5. Results and Discussion

The effects of different flow parameters on velocity, microrotation, temperature profile skin friction, wall couple stress and Nusselt number are analyzed through graphs and tables. A common feature of all the velocity profiles, is that the symmetrical inverted boundary layers are formed about the line x=0 in case of shrinking. As a result of which the effects of charecterising parameters M, K, α and β are opposite to that of the case of stretching, except the parameters Pr, f_w and λ (where the magnitudes are to be considered) and hence it is tacitly expressed by omitting the profiles for the case of shrinking.

5.1 Effect of flow parameters on velocity profile

Fig. 2 shows the effects of magnetic parameter (M) and material parameter (K) on the velocity distribution. It is observed that the effect of magnetic parameter is to decelerate the velocity whereas material parameter is to enhance it. Thus, it is to note that the material parameter representing the micropolar fluidity favors the growth of the boundary layer; consequently, the momentum transport gets diffused within the boundary layer.
Fig. 3 shows that higher value of Prandtl number (Pr) is to reduce the velocity in the flow domain due to low thermal conductivity which slows down the process of momentum transport for both stretching as well as shrinking of the plate.

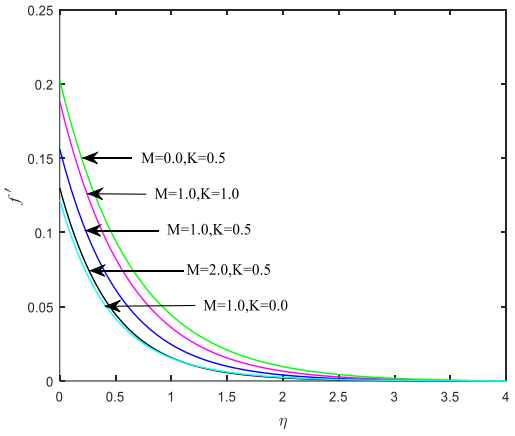

Fig. 2: Effect of M and K on f'

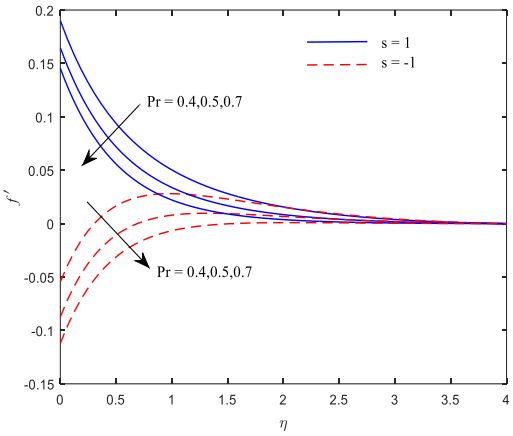

Fig. 3: Effect of Pr on f'

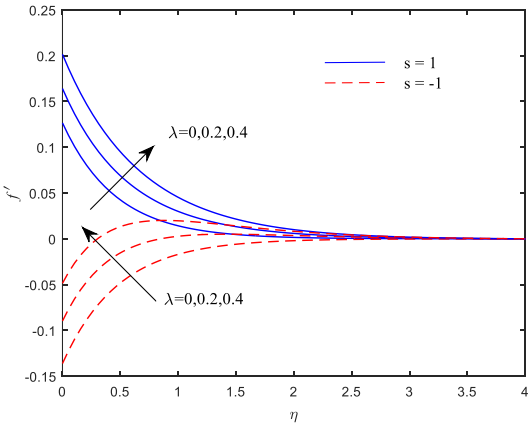

Fig. 4: Effect of λ on f'

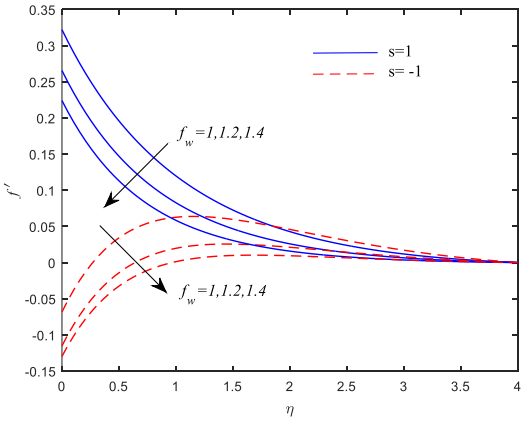

Fig. 5: Effect of f_w on f'

Fig. 4 shows the effect of buoyancy parameter (λ). This is an important parameter presenting the coupling effect of Grashof number and Reynolds number. When $\lambda < 1$ (under the predominance of Local Reynolds number), this parameter has an accelerating effect on the velocity field contributing to growth of boundary layer

in case of both stretching and shrinking. The accelerating effect can be attributed to the overpowering of inertia force over buoyancy force.
Fig. 5 shows the effect of suction at the plate. It is seen that for higher suction, the growth of boundary layer thickness decreases in case of stretching as well as shrinking. Due to higher suction, the decelerated fluid particles are removed and the thickness of boundary layer decreases.
Fig.6 shows the effects of first and second order slips on velocity profiles in case of stretching. It is seen that an increase in the first order slip decreases the momentum transport and hence velocity decreases producing thinner boundary layer. For second order slip, the curvature effect on the velocity profiles decreases.

5.2 Effect of flow parameters on temperature profile

Figs 7 and 8 show the effect of *Pr* and *Ec* on temperature profile. The increase in *Pr* (lower thermal conductivity) results in decrease of temperature distribution. Moreover, the Eckert number *Ec*, being a measure of addition of heat due to viscous dissipation enhances the temperature at all points for both stretching/shrinking of sheets. Further, it is seen that shrinking slightly enhances the temperature compared to the case of stretching.

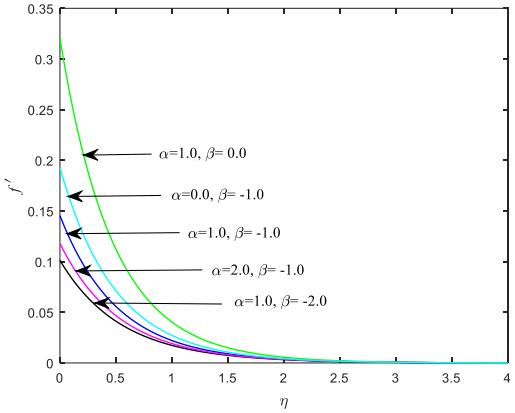

Fig. 6: Effect of α and β on f'

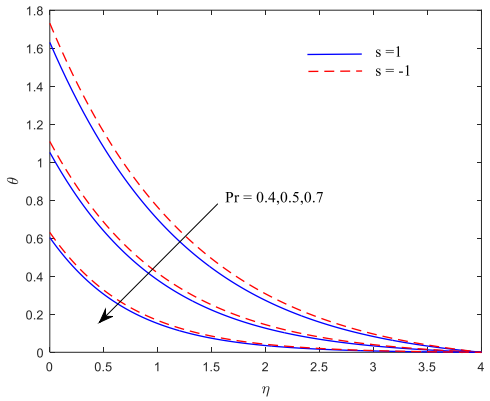

Fig. 7: Effect of *Pr* on θ

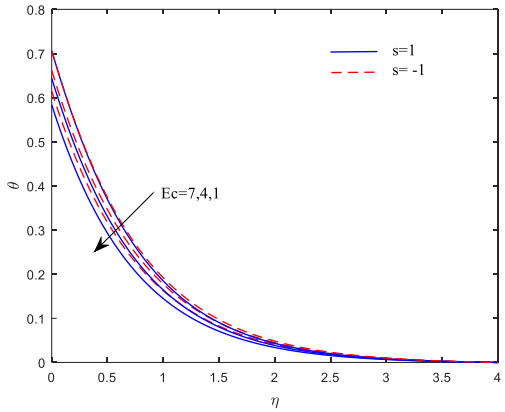

Fig. 8: Effect of *Ec* on θ

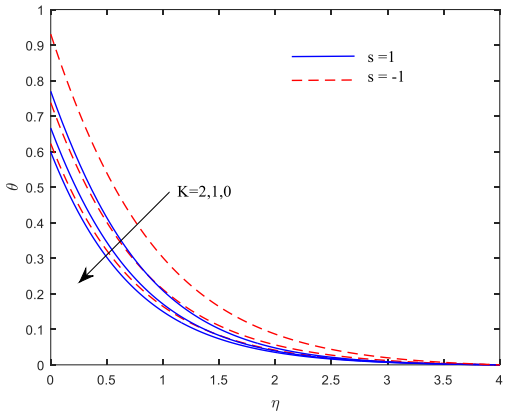

Fig. 9: Effect of *K* on θ

Figs 9 and 10 show the effects of material parameter (*K*) and magnetic parameter (*M*) on temperature distribution. It is seen that the effect of rheological property of micropolar fluid (*K*) is more pronounced in case of shrinking. From fig.10 it is observed that temperature decreases as the magnetic parameter increases in case of shrinking where the reverse effect is observed in case of stretching insignificantly.
Figs 11 and 12 show the effects of volumetric heat source and the Newtonian heating at the bounding surface. The effect of the heat source parameter, (Q>0) is to enhance the temperature, whereas, sink (Q<0) is to reduce it. Moreover, decrease in Newtonian heating parameter δ (which is proportional to the ratio of heat transfer h_s and thermal conductivity k at the solid surface expresses the relative importance of heat transport processes in two mediums i.e. solid and fluid) decreases the temperature distribution at all the layers for both stretching and shrinking. In case of shrinking little higher temperature distribution is indicated. The heat transfer process is

smooth in case of heat source whereas in case of Newtonian heating it is a little bit faster i.e. thermal transport process gets quicker.

5.3 Effect of flow parameters on microrotation profile

Fig. 13 shows the effect of magnetic parameter (*M*) and material parameter (*K*) on microrotation. It is observed that slight increase in magnetic parameter does not affect microrotation whereas increase in material parameter increases the microrotation significantly in case of shrinking.

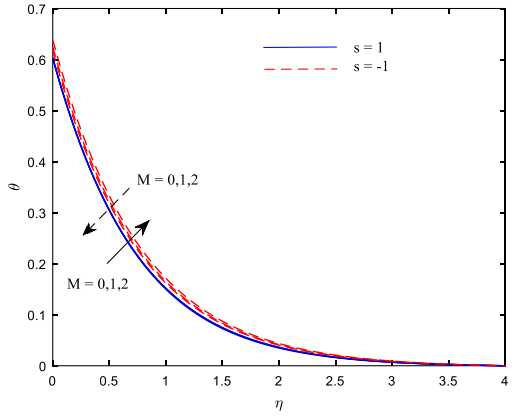

Fig. 10: Effect of *M* on θ

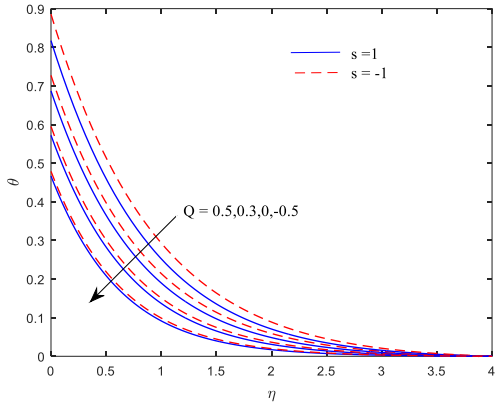

Fig. 11: Effect of Q on θ

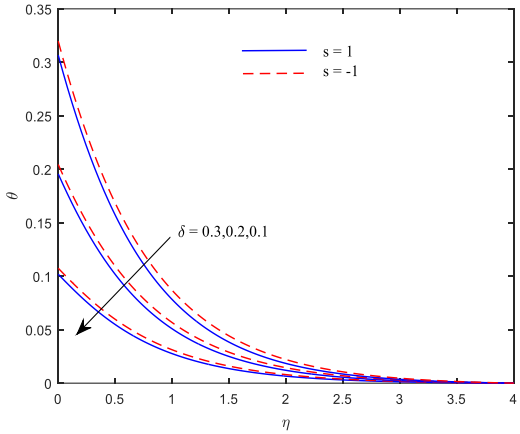

Fig. 12: Effect of δ on θ

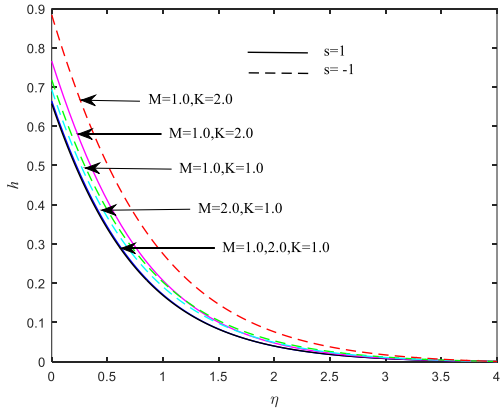

Fig. 13: Effect of *M* and *K* on *h*

5.4 Effect of flow parameters on skin friction, couple stress and Nusselt number

One of our profound interests in the present study is to analyze the surface criteria such as skin friction, couple stress and Nusselt number bearing the Rheological property of the fluid model considered herein. Tables 1 and 2 present the cases of stretching (s>0) and shrinking (s<0) of the sheet respectively. From Table 1 one important observation is that the Reynolds analogy holds good (Schlichting and Gersten, 1999), i.e., the parameter which increases the skin friction, one would expect that, for that parameter Nusselt number also increases which serves as the benchmark of validity. The deviation is marked in case of Newtonian heating parameter (δ) only. From Table 1 it is observed that skin friction increases as magnetic parameter (*M*), Prandtl number (*Pr*), suction (f_w), first order slip parameter (α) and strength of concentration of microelements (*n*) assume higher values, whereas, reverse effect is observed in the case of material parameter (*K*), buoyancy parameter (λ), second order slip parameter (β), heat generation/absorption parameter (*Q*), Newtonian heating parameter (δ) and Eckert number (*Ec*). The physical interpretation runs as: the magnetic parameter offers a resistive force to the primary flow and hence generates a higher shearing effect producing higher force coefficient at the stretching

surface. A similar explanation could be attributed to *Pr* also. The fluid with higher value of *Pr*, lowers down the thermal conductivity. In case of suction parameter, thinning of the boundary layer is a consequence and first order slip $(\alpha > 0)$, reduces boundary layer thickness. As expected a higher force coefficient is not a desirable outcome of the flow model, if not otherwise required. On the other hand, material parameter *K* is inversely proportional to fluid viscosity, and so as to enhance the flow, experiencing low shearing effect on the boundary and hence reducing the skin friction. A similar explanation can be attributed to the other parameters. Therefore, it is suggested that, these parameters adequately serve as input for obtaining lower skin friction. Further, Table 1 enumerates the values of wall couple stress and Nusselt number also. Here, all the entries are positive, unlike skin friction. The wall couple stress gets depleted with increasing values of *M*, *Pr* and α whereas, enhanced with *K*, λ, f_w, β, *Q*, *n*, *Ec* and δ. It is observed that as magnetic parameter *M* increases, couple stress experienced at the bounding surface decreases. This shows that in the presence of a resistive force due to the applied magnetic field, the velocity of the fluid flow decreases and hence the couple stress exerted at the bounding surface decreases. In the same way, we can explain the cases of *Pr* and α. Looking for the effect of other parameters such as *K*, λ, f_w, β, *Q*, *n*, *Ec* and δ on the wall couple stress, it is reported that, those parameters have a constructive impact to generate higher couple stress at the wall.

The effects of the parameters on Nusselt number, the rate of heat transfer coefficient are as follows. In view of Reynolds analogy between skin friction and Nusselt number, the effects are to be the same. Since the thermal boundary layer has a layered structure just as the velocity boundary layer, the parameters which contribute to a higher rate of heat transfer coefficient at the stretching surface, contribute to an enhanced Nusselt number. Moreover, as all the entries are positive, it indicates the heat flows from the plate to the fluid. It may cause thermal destabilizing effect in the flow domain.

Table 1: Effect of different parameters on skin friction, wall couple stress and Nusselt number for stretching sheet (s= 1)

M	*Pr*	*K*	λ	f_w	α	β	*Q*	*n*	δ	*Ec*	$C_{fx}Re_x^{1/2}$	$M_x\,Re_x$	$Nu_x\,Re_x^{-1/2}$
0.0	0.71	0.1	0.1	2.0	1.0	-1.0	0.1	0.5	0.5	0.0	-0.31009	0.30694	1.41261
1.0	0.71	0.1	0.1	2.0	1.0	-1.0	0.1	0.5	0.5	2.0	-0.28646	0.28251	1.34627
1.5	0.71	0.1	0.1	2.0	1.0	-1.0	0.1	0.5	0.5	2.0	-0.27696	0.27288	1.34719
1.0	2.00	0.1	0.1	2.0	1.0	-1.0	0.1	0.5	0.5	2.0	-0.28227	0.27811	3.50104
1.0	0.71	0.5	0.1	2.0	1.0	-1.0	0.1	0.5	0.5	2.0	-0.36529	0.31158	1.31498
1.0	0.71	0.1	0.5	2.0	1.0	-1.0	0.1	0.5	0.5	2.0	-0.31698	0.31467	1.32081
1.0	0.71	0.1	0.1	3.0	1.0	-1.0	0.1	0.5	0.5	2.0	-0.23932	0.34516	2.06123
1.0	0.71	0.1	0.1	2.0	2.0	-1.0	0.1	0.5	0.5	2.0	-0.22662	0.22212	1.36054
1.0	0.71	0.1	0.1	2.0	1.0	-2.0	0.1	0.5	0.5	2.0	-0.18416	0.17963	1.36851
1.0	0.71	0.1	0.1	2.0	1.0	-1.0	0.5	0.5	0.5	2.0	-0.28781	0.28403	1.12651
1.0	0.71	0.1	0.1	2.0	1.0	-1.0	0.1	1.0	0.5	2.0	-0.26864	0.56765	1.34843
1.0	0.71	0.1	0.1	2.0	1.0	-1.0	0.1	0.5	1.0	2.0	-0.31117	0.30841	1.39556
1.0	0.71	0.1	0.1	2.0	1.0	-1.0	0.1	0.5	0.5	3.0	-0.28665	0.28271	1.32083

Table 2 shows the case of shrinking sheet when s = -1. It is seen that the skin friction decreases with higher values of the parameters *M*, α, λ, f_w, *Q*, *n*, *Ec* and δ, a desirable outcome for the flow stability. On the other hand, *Pr*, *K* and β affect adversely. On comparing Table 1 with Table 2, it is observed that the effects of *Pr*, λ *Q*, δ and *Ec* remains same irrespective of stretching/shrinking, whereas, the other parameters such as *M*, *K*, f_w, α, β and *n* have the opposite effect. Considering the effect of couple stress, it is stated as follows: the effects of *Pr*, λ, *Q*, δ and *Ec* remain same as that of stretching but the other parameters have the opposite effect. Most interestingly, in case of shrinking, the Reynolds analogy holds good (Schlichting and Gersten (1999)) only for the parameters *Pr*, *Ec* and *Q* where as in case of other parameters it fails.

Table 3 presents a comparison of the present work with that of Ibrahim (2017) in case of a first order slip at the boundary (in the absence of second order slip). This shows that the present work is in good agreement with earlier ones.

Table 2: Effect of different parameters on Skin friction, Wall couple stress and Nusselt number for shrinking sheet (s= -1).

M	Pr	K	λ	f_w	α	β	Q	n	δ	Ec	$C_{fx}Re_x^{1/2}$	$M_x\,Re_x$	$Nu_x\,Re_x^{-1/2}$
0.0	0.71	0.1	0.1	2.0	1.0	-1.0	0.1	0.5	0.5	0.0	0.30017	-0.27871	1.34838
1.0	0.71	0.1	0.1	2.0	1.0	-1.0	0.1	0.5	0.5	2.0	0.27535	-0.26026	1.31741
1.5	0.71	0.1	0.1	2.0	1.0	-1.0	0.1	0.5	0.5	2.0	0.26622	-0.25284	1.32310
1.0	2.00	0.1	0.1	2.0	1.0	-1.0	0.1	0.5	0.5	2.0	0.28050	-0.26247	3.43545
1.0	0.71	0.5	0.1	2.0	1.0	-1.0	0.1	0.5	0.5	2.0	0.35880	-0.29438	1.27393
1.0	0.71	0.1	0.5	2.0	1.0	-1.0	0.1	0.5	0.5	2.0	0.24229	-0.23911	1.35654
1.0	0.71	0.1	0.1	3.0	1.0	-1.0	0.1	0.5	0.5	2.0	0.23105	-0.32886	2.04919
1.0	0.71	0.1	0.1	2.0	2.0	-1.0	0.1	0.5	0.5	2.0	0.21661	-0.20614	1.33771
1.0	0.71	0.1	0.1	2.0	1.0	-2.0	0.1	0.5	0.5	2.0	0.16293	-0.15612	1.35313
1.0	0.71	0.1	0.1	2.0	1.0	-1.0	0.5	0.5	0.5	2.0	0.27331	-0.26003	1.08714
1.0	0.71	0.1	0.1	2.0	1.0	-1.0	0.1	1.0	0.5	2.0	0.25811	-0.52345	1.32216
1.0	0.71	0.1	0.1	2.0	1.0	-1.0	0.1	0.5	1.0	2.0	0.24547	-0.24120	1.37184
1.0	0.71	0.1	0.1	2.0	1.0	-1.0	0.1	0.5	0.5	3.0	0.27518	-0.26017	1.29918

Table 3: Comparison of values of $f''(0)$ with 1st order slip flow parameter α when $M=\beta=Ec=f_w=Q=0$ and s=1,n=0.5, K=0, Pr=1

α	Present result	Ibrahim (2017)
0.0	1.004250	1.000000
0.1	0.876080	0.872082
0.2	0.780165	0.776377
0.3	0.705160	0.701548
0.5	0.594521	0.591196
1.0	0.432990	0.430160
2.0	0.286229	0.283980
3.0	0.215953	0.214055
5.0	0.146312	0.144841
10.0	0.082209	0.081243
20.0	0.044369	0.043790

6. Conclusions

i. Only inverted velocity boundary layers are formed for shrinking (baring thermal boundary layer), resulting opposite effects of the parameters to that of stretching.
ii. The material parameter representing the polar fluidity favors the growth of boundary layer; consequently, the momentum transport gets diffused within the boundary layer.
iii. The thermal buoyancy overpowers the inertia force.
iv. The higher order slip slows down the velocity and contributes to thinner boundary layer.
v. The material property and heat source contribute to thicker thermal boundary layer.
vi. Newtonian heating and microrotation enhance the micro fluid temperature under shrinking.
vii. As the magnitudes of second order slip increases, the magnitudes of skin friction and wall couple stress decreases but Nusselt number increases. Hence, the second order slip is favorable for stabilizing the velocity boundary layer and imposes a cooling effect on deformable surface.
viii. The skin friction increases (progressive thinning of boundary layer) with the increase in the value of magnetic parameter and Prandtl number.

Acknowledgement:

The authors thank the reviewers for their valuable comments which enriched the standard of the paper.

References

Ahmad, K., Ishak, A. and Nazar, R. (2013): Micropolar fluid flow and heat transfer over a nonlinearly stretching plate with viscous dissipation, Mathematical Problems in Engineering, Vol.2013, pp.1-5. http://dx.doi.org/ 10.1155/ 2013/257161

Animasaun, I.L. (2017): Melting heat and mass transfer in stagnation point micropolar fluid flow of temperature dependent fluid viscosity and thermal conductivity at constant vertex viscosity, J. Egypt. Math. Soc., Vol.25, No.1, pp.79-85. doi:10.1016/j.joems.2016.06.007

Aurangzaib, Md., Uddin, S., Bhattacharyya, K. and Shafie, S. (2016): Micropolar fluid flow and heat transfer over an exponentially permeable shrinking sheet, Propulsion and Power Research, Vol.5, No.4, pp.310-317. doi: 10.1016/j.jppr.2016.11.005

Baitharu, A.P., Sahoo, S.N. and Dash, G.C. (2020): Heat and mass transfer effect on a radiative second grade mhd flow in a porous medium over a stretching sheet, Journal of Naval Architecture and Marine Engineering, Vol.17, No.1, pp.51-66. http://dx.doi.org/10.3329/jname.v17i1.37777

Bakar, A.A. (2011): Effects of chemical reaction on MHD free convection and mass transfer flow of a micropolar fluid with oscillatory plate velocity heat and constant source in a rotating frame of reference, Commun Nonlinear Sci Numer Simulat, Vol.16, No.2, pp.698-710. https://doi.org/10.1016/j.cnsns.2010.04.040

Beavers, G.S. and Joseph, D.D. (1967): Boundary conditions at a natural permeable wall, J. Fluid Mech., Vol.30, pp.197-207. DOI: https://doi.org/10.1017/S0022112067001375

El-Aziz, M.A. (2013): Mixed convection flow of a micropolar fluid from an unsteady stretching surface with viscous dissipation, J. Egypt. Math. Soc., Vol.21, No.3, pp.385-394. https://doi.org/10.1016/j.joems.2013.02.010

Ibrahim, W. (2017): MHD Boundary layer flow and heat transfer of micropolar fluid past a stretching sheet with second order slip, Journal of the Brazilian Society of Mechanical Sciences and Engineering, Vol.39, No.3, pp.791-799. https://doi.org/10.1007/s40430-016-0621-8

Kamran, M. (2018): Heat source/sink and Newtonian heating effects on convective micropolar fluid flow over a stretching/shrinking sheet with slip flow model, International Journal of Heat and Technology, No.36, No.2, pp.473-482. https://doi.org/10.18280/ijht.360212

Kamran, M. and Wiwatanapataphee, B. (2018): Chemical Reaction and Newtonian Heating effects on steady convection flow of a micropolar fluid with second order slip at the boundary, European Journal of Mechanics B/Fluids, Vol.71, pp.138-150. 10.1016/j.euromechflu.2018.04.005

Khan, M., Rasheed, A., Ali, S. and Azim, Q.A. (2021): A novel formulation of 3D Jeffery fluid flow near an irregular permeable surface having chemical reactive species, Advances in Mechanical Engineering, Vol.13, No.5, pp.1–11. doi:10.1177/16878140211013609

Khan, M., Rasheed, A. and Salahuddin, T. (2020): Radiation and chemical reactive impact on tangent hyperbolic fluid flow having double stratification, AIP Advances Vol.10, pp.1-7. doi: 10.1063/5.0003717

Mahapatra, T.R., Dholey, S. and Gupta, A.S. (2007): Momentum and heat transfer in the magneto hydrodynamic stagnation-point flow of a viscoelastic fluid toward a stretching surface, Meccanica, Vol.42, No.3, pp.263-272. https://doi.org/10.1007/s11012-006-9040-8

Mahapatra, T.R. and Gupta, A.S. (2002): Heat transfer in stagnation-point flow towards a stretching sheet, Heat and Mass transfer, Vol.38, pp.517-521. https://doi.org/10.1007/s002310100215

Mahmoud, M.A.A. and Waheed, S.E. (2012): MHD flow and heat transfer of a micropolar fluid over a stretching surface with heat generation (absorption) and slip velocity, J. Egypt. Math. Soc., Vol.20, No.1, pp.20-27. https://doi.org/10.1016/j.joems.2011.12.009

Mebarek-Oudina, F., Aissa, A., Mahanthesh, B. and Öztop, Hakan F. (2020): Heat transport of magnetized Newtonian nanoliquids in an annular space between porous vertical cylinders with discrete heat source, International Communications in Heat and Mass Transfer, Vol.117, pp.1-8. https://doi.org/10.1016/j.icheatmasstransfer.2020.104737

Mishra, J.C. and Sinha, A. (2013): Effect of thermal radiation on MHD flow of blood and heat transfer in a permeable capillary in stretching motion, Heat and Mass transfer, Vol.49, pp.617-628. https://doi.org/10.1007/s00231-012-1107-6

Pal, D. and Mandal, G. (2017): Thermal radiation and MHD effects on boundary layer flow of micropolar nanofluid past a stretching sheet with non-uniform heat source/sink, International Journal of Mechanical Sciences, Vol.126, pp.308-318. https://doi.org/10.1016/j.ijmecsci.2016.12.023

Pal, D. and Mondal, H. (2010): Effect of variable viscosity on MHD non-Darcy mixed convective heattransfer over a stretching sheet embedded in a porous medium with non-uniform heat source/sink, Commun Nonlinear Sci Numer Simulat., Vol.15, No.6, pp.1553-1564. DOI: 10.1016/j.cnsns.2009.07.002

Pothanna, N. and Aparna, P. (2019): Unsteady thermo-viscous flow in a porous slab over an oscillating flat plate, Journal of porous media, Vol.22, No.5, pp.531-543. DOI:10.1615/JPorMedia.2019028871

Pothanna, N., Aparna, P. and Gorla, R.S.R. (2017): A numerical study of coupled non-linear equations of thermo-viscous fluid flow in cylindrical geometry, Int. J. of Applied Mechanics and Engineering, Vol.22, No.4, pp.965-979. DOI: https://doi.org/10.1515/ijame-2017-0062

Pothanna, N., Aparna, P. and Srinivas, J. (2016): Unsteady forced oscillations of a fluid bounded by rigid bottom, International Journal of Control Theory and Applications, Vol.9, No.19, pp. 9049-9054. https://www.researchgate.net/publication/313402079

Rout, P.K., Sahoo, S.N., Dash, G.C. and Mishra, S.R. (2016): Chemical reaction effect on MHD free convection flow in a micropolar fluid, Alexandria Engineering Journal, Vol.55, No.3, pp.2967-2973. https://doi.org/10.1016/j.aej.2016.04.033

Rosca, N.C. and Pop, I. (2013): Mixed convection stagnation point flow past a vertical flat plate with a second order slip: heat flux case, International Journal of Heat and Mass Transfer, Vol.65, pp.102-109. https://doi.org/10.1016/j.ijheatmasstransfer.2013.05.061

Sahoo, S.N. and Dash, G.C. (2012): Heat and mass transfer of MHD convective boundary layer flow past stretching porous wall embedded in a porous medium, Journal of Engineering Thermophysics, Vol.21, No.3, pp.181-192. DOI: 10.1134/S1810232812030034

Sharma, R., Ishak, A. and Pop, I. (2016): Stagnation Point flow of a micropolar fluid over a stretching/shrinking sheet with second order velocity slip, Journal of Aerospace Engineering, Vol. 29, No.5, pp.1-8. https://doi.org/10.1061/(ASCE)AS.1943-5525.0000616

Schliching, H. and Gersten, K. (1999): Boundary Layer Theory, Springer, 8th edition

Sheri, S.R. and Shamshuddin, M.D. (2015): Heat and mass transfer on the MHD flow of micropolar fluid in the presence of viscous dissipation and chemical reaction, Procedia Engineering, Vol.127, pp.885-892. https://doi.org/10.1016/j.proeng.2015.11.426

Swain, K., Mebarek‐Oudina, F., Abo‐Dahab, S. M. (2021): Influence of *MWCNT*/Fe_3O_4 hybrid nanoparticles on an exponentially porous shrinking sheet with chemical reaction and slip boundary conditions, Journal of Thermal Analysis and Calorimetry, https://doi.org/10.1007/s10973-020-10432-4

Turkyilmazoglu, M. (2014): A note on micropolar fluid flow and heat transfer over a porous shrinking sheet, International Journal of Heat and Mass Transfer, Vol.72, pp.388-391. https://doi.org/10.1016/j.ijheatmasstransfer.2014.01.039